38. Wen PY, Macdonald DR, Reardon DA, et al. Update response assessment criteria for high-grade gliomas: Response Assessment in Neuro-Oncology Working Group. *J Clin Oncol* 2010;28:1963–72.
39. Vredenburgh JJ, Cloughesy T, Samantc M, et al. Corticosteroid use in patients with glioblastoma at first or second relapse treated with bevacizumab in the BRAIN study. *Oncologist* 2010;15:1329–34.
40. Chamberlain MC, Johnston SK. Salvage therapy with single-agent bevacizumab for recurrent glioblastoma. *J Neurooncol* 2010;96:259–69.
41. *A Study of Avastin (bevacizumab) in Combination with Temozolomide and Radiotherapy in Patients with Newly Diagnosed Glioblastoma [Internet]*. USA: Clinicaltrials.gov, 2009 (cited 4 October 2011). http://clinicaltrials.gov/ct2/show/NCT00943826.
42. *Temozolomide and Radiation Therapy with or Without Bevacizumab in Treating Patients with Newly Diagnosed Glioblastoma [Internet]*. USA: Clinicaltrials.gov, 2009 (cited 4 October 2011). http://clinicaltrials.gov/ct2/show/NCT00884741.
43. Van Meir EG, Hadjipanayis CG, Norden AD, et al. Exciting new advances in neuro-oncology: the avenue to a cure for malignant glioma. *CA Cancer J Clin* 2010;60:166–93.

Cancer Science
The official journal of the Japanese Cancer Association JCA

Significance of *IDH* mutations varies with tumor histology, grade, and genetics in Japanese glioma patients

Akitake Mukasa,[1,9] Shunsaku Takayanagi,[1] Kuniaki Saito,[1] Junji Shibahara,[2] Yusuke Tabei,[3] Kazuhide Furuya,[4] Takafumi Ide,[5] Yoshitaka Narita,[6] Ryo Nishikawa,[7] Keisuke Ueki[8] and Nobuhito Saito[1]

Departments of [1]Neurosurgery, [2]Pathology, University of Tokyo, Tokyo; [3]Department of Neurosurgery, Tokyo Metropolitan Cancer and Infectious Diseases Center Komagome Hospital, Tokyo; [4]Department of Neurosurgery, Teikyo University School of Medicine, Tokyo; [5]Department of Neurosurgery, Tokyo Metropolitan Bokutoh Hospital, Tokyo; [6]Department of Neurosurgery and Neuro-Oncology, National Cancer Center Hospital, Tokyo; [7]Department of Neuro-Oncology/Neurosurgery, International Medical Center, Saitama Medical University, Saitama; [8]Department of Neurosurgery, Dokkyo University School of Medicine, Tochigi, Japan

(Received October 20, 2011/Revised November 24, 2011/Accepted November 29, 2011/Accepted manuscript online December 2, 2011/Article first published online January 13, 2012)

Mutations in isocitrate dehydrogenase 1 (*IDH1*) and *IDH2* are found frequently in malignant gliomas and are likely involved in early gliomagenesis. To understand the prevalence of these mutations and their relationship to other genetic alterations and impact on prognosis for Japanese glioma patients, we analyzed 250 glioma cases. Mutations of *IDH1* and *IDH2* were found in 73 (29%) and 2 (1%) cases, respectively. All detected mutations were heterozygous, and most mutations were an Arg132His (G395A) substitution. *IDH* mutations were frequent in oligodendroglial tumors (37/52, 71%) and diffuse astrocytomas (17/29, 59%), and were less frequent in anaplastic astrocytomas (8/29, 28%) and glioblastomas (13/125, 10%). The pilocytic astrocytomas and gangliogliomas did not have either mutation. Notably, 28 of 30 oligodendroglial tumors harboring the 1p/19q co-deletion also had an *IDH* mutation, and these alterations were significantly correlated ($P < 0.001$). The association between *TP53* and *IDH* mutation was significant in diffuse astrocytomas ($P = 0.0018$). *MGMT* promoter methylation was significantly associated with *IDH* mutation in grade 2 ($P < 0.001$) and grade 3 ($P = 0.02$) gliomas. *IDH* mutation and 1p/19q co-deletion were independent favorable prognostic factors for patients with grade 3 gliomas. For patients with grade 3 gliomas and without 1p/19q co-deletion, *IDH* mutation was strongly associated with increased progression-free survival ($P < 0.0001$) and overall survival ($P < 0.0001$), but no such marked correlation was observed with grade 2 gliomas or glioblastomas. Therefore, *IDH* mutation would be most useful when assessing prognosis of patients with grade 3 glioma with intact 1p/19q; anaplastic astrocytomas account for most of these grade 3 gliomas. (*Cancer Sci* 2012; 103: 587–592)

Gliomas are among the most common and formidable brain tumors.[1] Despite intensive treatment, most patients die within 2-10 years. Therefore, development of novel therapeutic strategies based on greater understanding of tumor characteristics is needed. Recently, a comprehensive sequence analysis of human GBM that included most human genes revealed frequent mutations in *IDH1*.[2] Subsequent analyses revealed that these mutations occur more frequently in low-grade glioma than in GBM, with a rate of *IDH1* mutation as high as 59–90%.[3–7] The *IDH* gene mutation is currently believed to occur in the early stage of gliomagenesis[4,6] and to play a critical role in tumor development.

The *IDH* genes encode redox enzymes; these enzymes convert isocitrate to alpha-ketoglutarate, use NAD(P)+ as a coenzyme, and function in energy metabolism. There are three *IDH* genes in humans, and only mutations in *IDH1* are frequently found in gliomas; the IDH1 enzyme resides in the cytosol and peroxisomes.[2–7] Mutations in *IDH2* are rare in gliomas; IDH2 localizes to mitochondria and functions in the Krebs (citric acid) cycle. To date, no *IDH3* mutation has been reported. Most *IDH1* mutations in gliomas are missense mutations at amino acid 132, which is in the catalytic domain and binds to substrate. Similarly, *IDH2* mutations in gliomas are substitutions at amino acid 172, which is functionally equivalent to amino acid 132 of IDH1. *IDH1* and *IDH2* mutations in the catalytic domain are also found in 8–23% of acute myeloid leukemias.[8,9] Mutations in *IDH* genes are rarely found in other tumors.[7,10]

In general, a tumor with an *IDH* mutation has either an *IDH1* or *IDH2* mutation, and the mutation is heterozygous with a wild-type allele.[2,4,6,7] This observation led to the notion that mutated *IDH1/IDH2* genes gain novel functions and are oncogenes, and that the wild-type *IDH* genes are not tumor suppressor genes. In fact, mutant IDH1 has novel enzymatic activity; it converts alpha-ketoglutarate to 2-HG, and accumulated 2-HG is presumed to contribute to tumorigenesis as an "oncometabolite".[9,11–13]

Malignant gliomas categorized as WHO grade 4[2,5,7,14,15] or grade 3[5,7,15–17] with an *IDH* mutation were reportedly associated with higher PFS[15–17] and OS[2,5,7,14–17] than those without an *IDH* mutation. However, for grade 2 gliomas, the relation between the presence of an *IDH* mutation and prognosis is controversial.[15,18–20]

The *IDH* mutations apparently have an important role in many aspects of glioma, including gliomagenesis, patient prognosis, and development of therapeutic strategies. However, information on *IDH* mutations in gliomas, such as prevalence, relation to other genetic alterations, and prognostic value, is still limited, particularly for Asian populations,[21,22] including Japanese patients.[5,17] Thus, to further clarify the significance of *IDH* mutations with regard to proper diagnosis and optimized treatment of malignant gliomas, we sought basic data on a large number of Japanese glioma patients for *IDH1* and *IDH2* mutations and other genetic and epigenetic alterations frequently found in gliomas, specifically 1p/19q LOH, *TP53* mutation, and *MGMT* promoter methylation.

Materials and Methods

Tumor specimens. Tumor samples and paired blood samples were obtained following surgery. Of 250 gliomas, 168 tumors were collected at the University of Tokyo hospital (Tokyo,

[9]To whom correspondence should be addressed.
E-mail: mukasa-nsu@umin.ac.jp

doi: 10.1111/j.1349-7006.2011.02175.x

Japan) and 82 gliomas were collected at collaborating hospitals. The study was approved by the Ethics Committee of the University of Tokyo and all patients gave written informed consent. Histological diagnoses were made on formalin-fixed, paraffin-embedded tissues following the WHO classification[1] by a neuropathologist (J.S.) for samples from the University of Tokyo hospital and consensus diagnoses were made by four neuropathologists for samples from other hospitals as reported previously.[23] Genomic DNA was extracted for genetic analyses. Patients with the same grade (2, 3, or 4) glioma were treated similarly with surgical resection followed by radiotherapy and alkylating agent chemotherapy.

Genetic analysis. For *IDH* gene mutations, the genomic regions spanning the catalytic domain of *IDH1*, including codon 132, and of *IDH2*, including codon 172, were analyzed by direct sequencing using the Genetic Analyzer 310 (Applied Biosystems, Foster City, CA, USA). An aliquot of DNA was amplified by PCR using AmpliTaq Gold (Applied Biosystems) with annealing temperature at 55°C. The primers 5′-TGCCACCAACGACCAAGTCA and 5′-TGTGTTGAGATGGACGCCTATTTG were used for *IDH1* amplification and sequencing, as reported previously.[15] Amplification of *IDH2* was carried out using the primers 5′-CTCTGTCCTCACAGAGTTCAAGC and 5′-CCACTCCTTGACACCACTGCC, and the *IDH2* sequencing reactions were carried out using the primers 5′-AAGTCCCAATGGAACTATCCG and 5′-TCTGTGGCCTTGTACTGCAGAG.

Loss of heterozygosity on chromosomes 1p and 19q was determined using microsatellite analysis as described previously.[23] When tumors had no available paired blood DNA or when the LOH assay was ambiguous because of non-informative microsatellite markers, MLPA assay was carried out using the SALSA MLPA kit P088 (MRC Holland, Amsterdam, the Netherlands) following the manufacturer's instructions. *TP53* gene mutation was determined by direct sequencing following PCR-SSCP screening of exons 5–8 of *TP53*, as described previously.[24]

Methylation-specific PCR. Genomic DNA samples (250 ng each) were used for bisulfite reactions using the EZ DNA Methylation Kit (Zymo Research, Irvine, CA, USA) according to the manufacturer's protocol. DNA methylation status of the *MGMT* promoter was then determined by methylation-specific PCR as described by Esteller *et al.*[25]

Statistical analysis. Fisher's exact test was used to compare the genotype distributions. Overall survival was defined as the time between initial surgery and death or last follow-up. Progression-free survival was defined as the time between initial surgery and recurrence or last follow-up. Both OS and PFS were calculated according to the Kaplan–Meier method, and differences among patient subsets were evaluated using the log–rank test. Statistical calculations were carried out using JMP 9 (SAS Institute, Cary, NC, USA).

Results

Frequency and characteristics of *IDH* mutations in glioma samples from Japanese patients. We analyzed 250 human glioma samples obtained following surgery; these tumors consisted of 125 GBM, 29 AA, 29 DA, 52 oligodendroglial tumors, 9 PA, and 6 GGL. Mutations of *IDH1* and *IDH2* were found in 73 (29%) and 2 (1%) tumors, respectively. All detected mutations were heterozygous, missense mutations. Among the 73 *IDH1* mutations, the G395A (R132H) substitution was the most frequent mutation (occurring in 70/73 cases, 96%), C394A (R132S) substitutions occurred in two cases, and a C394T (R132C) substitution occurred in one case. Of the two *IDH2* mutations, one was a G515A (R172K) substitution, and the other was an A514T (R172W) substitution. *IDH* mutations (*IDH1* or *IDH2*) were found in 13 (10%) of 125 GBM, 8 (28%) AA, 17 (59%) DA, and in 37 (71%) oligodendroglial tumors (Table 1). In the 52 oligodendroglial tumors, *IDH* mutations were found in 19/25 (76%) OG, 4/7 (57%) OA, 10/15 (67%) AOG, and 4/5 (80%) AOA. No mutation was detected in any case of PA or GGL. A higher rate of *IDH* mutation was found in secondary GBM (6/13, 46%) than primary GBM (6/109, 6%). In the three GBMO cases, there was only one *IDH1* mutation.

Association between *IDH* mutation and 1p/19q co-deletion, *TP53* mutation, or *MGMT* promoter methylation. The frequencies of 1p/19q co-deletion and *TP53* mutation and their relationship with *IDH* mutations are shown in Table 1. As expected, 1p/19q co-deletion was common in oligodendroglial tumors, especially those without an astrocytic component (OG 76%, AOG 67%), whereas *TP53* mutations were common in lower-grade astrocytomas (DA 45%); these genetic aberrations were never coincident. In OG, 1p/19q co-deletion was significantly correlated with *IDH* mutation ($P < 0.001$), and almost all oligodendroglial tumors with 1p/19q co-deletion had an *IDH* mutation (28/30, 93%).

The *TP53* mutation was more prevalent in DA (45%) than in AA (34%) or primary GBM (22%). However, when *IDH* mutation was present, *TP53* mutation was more frequent, and *TP53* mutations were found in 12/17 (71%) DA, 5/8 (63%) AA, and 3/6 (50%) primary GBMs that also had an *IDH* mutation. The rates of *IDH* mutation in astrocytic tumors with *TP53* mutation were higher than those with wild-type *TP53* (92% *vs* 31% in DA, 50% *vs* 16% in AA, and 13% *vs* 4% in primary GBM), and the association between *TP53* and *IDH* mutation was significant in DA ($P = 0.0018$), but not in AA or GBM. The majority of DA tumors with *TP53* mutation had *IDH* mutation (12/13, 92%); in contrast, only a few primary GBM tumors with *TP53* mutation also had an *IDH* mutation (3/23, 13%).

Of a total 250 gliomas, *MGMT* promoter methylation status was analyzed for 132 gliomas (grade 2, 3, and 4) resected at the University of Tokyo hospital. Methylation was evident in 37/69 GBM (54%), 5/18 AA (28%), 10/17 DA (59%), 8/10 AOG/AOA (80%), and 13/18 OG/OA (72%) (Table 1). The association between *IDH* mutation and *MGMT* methylation was significant in grade 2 ($P < 0.001$) and grade 3 gliomas ($P = 0.02$), but not in grade 4 gliomas ($P = 0.11$).

Prognostic value of *IDH* mutation and other genetic alterations. We evaluated the potential prognostic value of *IDH* mutation and other genetic alterations in WHO grade 2, 3, and 4 gliomas. For patients with grade 2 gliomas, univariate analysis showed that *IDH* mutation was not associated with OS ($P = 0.07$) or PFS ($P = 0.29$). Codeleted 1p/19q and wild-type *TP53* each slightly correlated with increased PFS ($P = 0.014$ and $P = 0.029$, respectively), but they were not correlated with OS, and neither of these genetic alterations showed significant association with prognosis in multivariate analysis (Table 2). *MGMT* promoter methylation was also not associated with prognosis. Similarly, we did not observe a significant association of *IDH* mutation with better prognosis for DA (OS, $P = 0.10$; PFS, $P = 0.58$).

In grade 3 gliomas, univariate analysis showed that the association between *IDH* mutation and prolonged survival (OS, $P = 0.0004$; PFS, $P < 0.0001$) was significant and that 1p/19q co-deletion was associated with prolonged survival (OS, $P = 0.028$; PFS, $P = 0.0025$), but that neither *TP53* mutation nor *MGMT* promoter status was associated with prognosis. Although *IDH* mutation and 1p/19q co-deletion were tightly associated with one another, the multivariate analysis further indicated that these alterations were independent indicators of a favorable prognosis (Table 2). *IDH* mutation was present in almost all tumors with the 1p/19q co-deletion.[26] Therefore, grade 3 gliomas were divided into three genetic subgroups: (i) 1p/19q codeleted tumors, most of which carry *IDH* mutation and show oligodendroglial phenotype; (ii) tumors without 1p/19q co-deletion and with mutant *IDH*; and (iii) tumors

doi: 10.1111/j.1349-7006.2011.02175.x

Table 1. *IDH* mutation and common genetic and epigenetic alterations in gliomas from Japanese patients

Tumor pathology (WHO grade) *IDH1* or *IDH2* status	No. of patients	Frequency of *IDH1* or *IDH2* mutation	Median age, years	Male sex (%)	1p/19q co-deletion	*TP53* mutation	Methylated *MGMT* promoter (%)
GBM primary (Gr. 4)	109	6/109 (6%)	62	61	1	23 (22%)	27/57 (47)
Mutant	6		43	50	1	3 n.s.	1/1 (100)
Wild-type	103		62	61	0	20	26/56 (46)
GBM secondary (Gr. 4)	13	6/13 (46%)	47	69	0	2 (15%)	7/9 (78)
Mutant	6		52	50	0	2 n.s.	4/5 (80)
Wild-type	7		43	86	0	0	3/4 (75)
GBMO (Gr.4)	3	1/3 (33%)	80	67	1	0	3/3 (100)
Mutant	1		62	100	1	0	1/1 (100)
Wild-type	2		80	50	0	0	2/2 (100)
Anaplastic astrocytoma (Gr. 3)	29	8/29 (28%)	57	55	1	10 (34%)	5/18 (28)
Mutant	8		46	50	1	5 n.s.	2/5 (40)
Wild-type	22		60	57	0	5	3/13 (23)
Anaplastic oligoastrocytoma (Gr. 3)	5	4/5 (80%)	43	40	0	4 (80%)	2/3 (66)
Mutant	4		48	25	0	3 n.s.	2/2 (100)
Wild-type	1		11	100	0	1	0/1 (0)
Anaplastic oligodendroglioma (Gr. 3)	15	10/15 (67%)	62	56	10 (67%)	0	6/7 (86)
Mutant	10		49	43	9*	0	5/5 (100)
Wild-type	5		66	100	1	0	1/2 (50)
Diffuse astrocytoma (Gr. 2)	29	17/29 (59%)	32	61	3	13 (45%)	10/17 (59)
Mutant	17		33	59	2	12***	10/10 (100)
Wild-type	12		30	64	1	1	0/7 (0)
Oligoastrocytoma (Gr. 2)	7	4/7 (57%)	44	71	1	1	5/6 (83)
Mutant	4		37	100	1	1	3/3 (100)
Wild-type	3		53	33	0	0	2/3 (67)
Oligodendroglioma (Gr. 2)	25	19/25 (76%)	46	52	19 (76%)	3	8/12 (66)
Mutant	19		47	53	18**	1	7/10 (70)
Wild-type	6		34	50	1	2	1/2 (50)
Pilocytic astrocytoma (Gr. 1)	9	0%	12	56	0	0	N/A
Mutant	0		N/A	N/A	0	0	
Wild-type	9		12	56	0	0	
Ganglioglioma (Gr. 1)	6	0%	22	67	0	0	N/A
Mutant	0		N/A	N/A	0	0	
Wild-type	6		22	67	0	0	

*P = 0.0037; **P = 0.0001; ***P = 0.0018. The association with *IDH* mutation (Fisher's exact test). GBM, glioblastoma; GBMO, glioblastoma with oligodendroglioma component; N/A, not analyzed; n.s., not significant.

Table 2. Prognostic value of common genetic alterations for overall survival (OS) and progression-free survival (PFS) in gliomas (multivariate analysis)

	PFS			OS		
	P-value	Hazard ratio	95% CI	*P*-value	Hazard ratio	95% CI
Grade 2 glioma						
IDH mutation	0.4408	0.602	0.1678–2.1535	0.1573	0.329	0.0728–1.5270
1p/19q co-deletion	0.3591	0.495	0.1083–2.2020	0.7988	1.237	0.2353–6.0194
TP53 mutation	0.2904	2.036	0.5526–7.7157	0.4693	0.537	0.0685–2.6350
Grade 3 glioma						
IDH mutation	<0.0001†	0.059	0.0086–0.2395	0.0403†	0.319	0.0985–0.9519
1p/19q co-deletion	0.0016†	0.055	0.0025–0.3904	0.0170†	0.184	0.0271–0.7567
TP53 mutation	0.4144	0.646	0.2045–1.7994	0.0300†	0.294	0.0786–0.8937
Primary GBM						
IDH mutation	0.8456	0.898	0.2575–2.4255	0.8560	0.905	0.2609–2.4203
TP53 mutation	0.1533	0.605	0.2792–1.1944	0.3089	0.705	0.3354–1.3613
Methylated *MGMT* promoter	0.0031†	0.407	0.2216–0.7375	0.0058†	0.429	0.2324–0.7820

†Significant value. Cox proportional hazard modeling for OS or PFS was applied for the major variable for prognostic factors. CI, confidence interval; GBM, glioblastoma.

without 1p/19q co-deletion and with wild-type *IDH*. Grade 3 gliomas were assessed with regard to the association between the genetic alterations and disease course (Fig. 1). In these genetic subgroups, grade 3 gliomas without 1p/19q co-deletion and with wild-type *IDH* were revealed to have markedly worse OS ($P < 0.0001$) (Fig. 1C) and PFS ($P < 0.0001$) (Fig. 1D), but

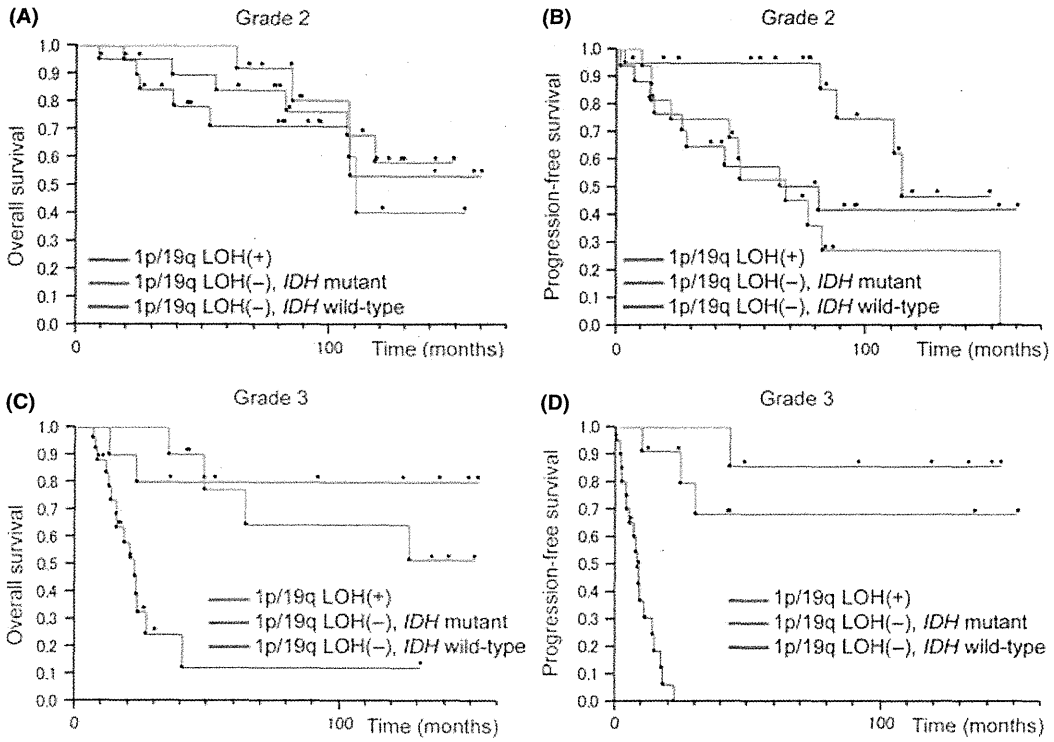

Fig. 1. Overall survival (OS) and progression-free survival (PFS) curves for patients with grade 2 and 3 gliomas with or without 1p/19q loss of heterozygosity (LOH) and/or isocitrate dehydrogenase (*IDH*) mutation. Overall survival (A) and PFS (B) in grade 2 gliomas; OS (C) and PFS (D) in grade 3 gliomas.

these lower survival rates were not observed for patients with grade 2 gliomas lacking 1p/19q co-deletion and *IDH* mutation (Fig. 1A,B). Grade 3 gliomas without 1p/19q co-deletion were predominantly AA (28 AAs, 5 AOAs, and 5 AOGs), and only 1 AA had the 1p/19q co-deletion (Table 1). The *IDH* mutation was significantly associated with increased OS ($P = 0.0064$) and PFS ($P = 0.0001$) for patients with AA based on the univariate analysis. *TP53* mutation was also correlated with increased PFS ($P = 0.013$), but *MGMT* promoter methylation showed no significant association with PFS or OS.

In primary GBM, our univariate analysis showed that neither *IDH* mutation, 1p/19q co-deletion, nor *TP53* mutation was associated with PFS or OS, but *MGMT* promoter methylation was significantly associated with increased OS ($P = 0.0043$) and PFS ($P = 0.0038$).

Discussion

Here we report that *IDH* mutation, which was tightly associated with 1p/19q co-deletion and *MGMT* promoter methylation, was common in grade 2 gliomas and also, but to a lesser extent, in grade 3 gliomas. Moreover, we found that *IDH* mutation would be an especially useful genetic marker for evaluating the malignancy of grade 3 gliomas that do not have a 1p/19q co-deletion and that these gliomas were predominantly AA.

The frequencies and patterns of *IDH* mutation in our glioma samples from Japanese patients were largely comparable to those in previous reports.[2–7] *IDH* mutation was found predominantly in grade 2 glioma, such as DA, OA, and OG. *IDH* mutation frequencies were lower in higher-grade gliomas, and less than 10% of GBM had an *IDH* mutation; however, nearly half of secondary GBM, which developed from malignant transformation of lower-grade glioma, had an *IDH* mutation. These observations supported the notion that the *IDH* mutation has a crucial role in the development of the majority of grade 2 gliomas. In grade 3 gliomas, the oligodendroglial tumors had higher frequency of *IDH* mutation than astrocytic tumors (OG 76% > DA 59%, $P = 0.18$; AOG 67% > AA 28%, $P < 0.05$; Pearson's chi-square-test). No *IDH* mutation was detected in any grade 1 glioma, PA or GGL; this observation indicated that these tumors had a different genetic etiology from that of grade 2 and 3 infiltrative astrocytic and oligodendroglial tumors. This observation also supported the usefulness of *IDH* mutations along with BRAF alterations for differential diagnosis of PA.[27] However, our results differed from two previous reports that detected *IDH1* mutation (8–38%) in GGL.[5,28] Further studies are needed to clarify the biological and clinical significance of *IDH1* mutation in GGL.

As reported previously,[23] *TP53* mutation and co-deletion of chromosomes 1p and 19q were frequent alterations in grade 2 and grade 3 gliomas. The 1p/19q co-deletions were mostly found in oligodendroglial lineage gliomas, whereas *TP53* mutations were more frequent in gliomas derived from the astrocytic lineage. *IDH* mutation is currently believed to precede 1p/19q LOH and *TP53* mutation during the early stage of gliomagenesis,[4,6] and consistent with this hypothesis, most of our grade 2 gliomas that had 1p/19q co-deletion or *TP53* mutations also harbored an *IDH* mutation. In one study, all the gliomas with deletions of the entire 1p and 19q arms carried an *IDH1* or *IDH2* mutation;[26] however, we found a few exceptions in which there was 1p/19q LOH, but no *IDH* mutation. These apparent exceptions might have been artifacts due to our imperfect methods for detecting the extent of 1p/19q LOH, specifically microsatellite analysis or MLPA; these methods do not effectively differentiate partial chromosomal loss from typical entire 1p/19q hemizygous deletion, which is generally found in OG harboring *IDH* mutation. It would be better to carefully evaluate the extent of 1p/19q LOH in such exceptional cases. *TP53* mutation was also

doi: 10.1111/j.1349-7006.2011.02175.x

associated with *IDH* mutation in DA. However, there was no association between *IDH* and *TP53* mutation in AA or primary GBM. This observation suggested that *TP53* mutation promoted tumor growth independently of *IDH* mutation, especially in higher grade gliomas. Most gliomas with an *IDH* mutation had either 1p/19q LOH or *TP53* mutation, further supporting the hypothesis that combinations of *IDH* mutation and subsequent genetic alteration are common pathways leading to low-grade glioma. However, there were also a few other *IDH*-mutated gliomas that had neither 1p/19q co-deletion nor *TP53* mutation. In these gliomas, the kind of alterations subsequent to *IDH* mutation that caused progenitor cells to give rise to low-grade glioma remains to be elucidated.

Methylation at the *MGMT* promoter was associated with *IDH* mutation, especially for low-grade gliomas. Some IDH enzymes with a mutation in the catalytic domain acquire a novel enzymatic activity[9,11] that causes accumulation of 2-HG, and 2-HG is known to inhibit enzymes such as 5-methylcytosine hydroxylases and histone demethylases. As a result, *IDH* mutations bring about genome-wide hypermethylation, which might lead to tumor initiation.[12,29] Reportedly, the majority of low-grade gliomas have hypermethylated CpG islands throughout the genome; this phenomenon is called the glioma CpG island methylator phenotype, and these tumors frequently harbor *IDH* mutation.[30–32] Therefore, frequent *MGMT* promoter methylation in *IDH*-mutated low-grade glioma was possibly simply a reflection of hypermethylation of a plethora of genes resulting from the methylator phenotype. In contrast, the majority of GBM had *MGMT* promoter hypermethylation without also having *IDH* mutation, indicating that *MGMT* promoter methylation occurs independent of *IDH*-related hypermethylation in most GBM. Probably because of such a background, the prognostic values of *MGMT* promoter methylation for *IDH*-mutated and *IDH*-wild-type gliomas are not equal. In GBM, *MGMT* promoter methylation is a predictive factor for the efficacy of temozolomide, which is a common alkylating agent used in the chemotherapeutic treatment of malignant glioma.[33,34] However, the predictive value of *MGMT* promoter methylation for chemosensitivity in grade 2 and grade 3 glioma is controversial.[19,35]

The prognostic significance of *IDH* mutation differed among WHO tumor grades. Unlike previous reports, *IDH* mutation was not associated with the PFS or OS of our GBM patients; however, this finding might result from insufficient numbers of GBM patients with *IDH* mutation. A methylated *MGMT* promoter, which reflects the sensitivity of a tumor to temozolomide, was associated with favorable PFS and OS for patients with GBM, further emphasizing the importance of detecting *MGMT* promoter methylation status in GBM.

Among patients with grade 2 gliomas, *IDH* mutation was also not associated with prognosis. Wild-type *TP53* and 1p/19q co-deletion were each associated with prolonged PFS, probably because these two genetic alterations were mutually exclusive and tumors with wild-type *TP53* likely have a 1p/19q co-deletion, which is a recognized favorable prognostic factor. The prognostic value and predictability of temozolomide efficacy associated with *IDH* mutation in low-grade gliomas has been controversial. Consistent with our results, Kim *et al.*[20] showed that *IDH1* and *IDH2* mutations are not prognostic in low-grade gliomas, but that *TP53* mutation is a significant prognostic indicator of shorter survival and 1p/19q loss is prognostic of longer survival. However, Sanson *et al.*[15] reported a different result, specifically that *IDH1* mutation is associated with a better outcome in grade 2 gliomas. Dubbink *et al.*[18] showed that *IDH* mutation is associated with better outcomes for relapsed astrocytomas previously treated with radiotherapy, but there was no relationship between *IDH* mutation and temozolomide responsiveness. Houillier *et al.*[19] showed that *IDH1* or *IDH2* mutations predict better prognosis of glioma treated with temozolomide, but they did not appear to influence the course of untreated low-grade glioma. Thus, the prognostic value of *IDH* mutation is different from that of 1p/19q co-deletion, which is prognostic as well as predictive for responsiveness to temozolomide in low-grade gliomas. These inconsistent results on the association between *IDH* mutation and survival in cases of low-grade gliomas might be caused by the variable numbers of OG and DA included in these studies. Almost all oligodendroglial tumors with 1p/19q co-deletion also have an *IDH* mutation;[26] therefore, many cases of OG with favorable prognoses may affect and confound measurements of survival rate in the whole group of low-grade gliomas with *IDH* mutations. To avoid the confounding influence of OG, we also focused on DA with wild-type *IDH*; these tumors generally have neither 1p/19q LOH nor *TP53*. However, they had outcomes comparable to those of DA with *IDH* mutation. This finding indicated that DA with wild-type *IDH* was not more malignant than DA with an *IDH* mutation. This observation differed from the observation that AA with wild-type *IDH* had markedly worse outcomes than AA with an *IDH* mutation (OS, $P = 0.0064$; PFS, $P = 0.0001$).

In contrast with grade 2 and 4 gliomas, the prognostic significance of *IDH* mutation was evident for grade 3 gliomas, and this finding was consistent with previous reports.[15,17,36] Almost all gliomas with 1p/19q co-deletion have an *IDH* mutation,[26] and anaplastic oligodendroglial tumors often harbor 1p/19q co-deletion; therefore, monitoring of *IDH* mutation might have more clinical significance for patients with grade 3 gliomas with intact 1p/19q, and these tumors are predominantly AA. In fact, as the histopathological differential diagnosis of AA from GBM or DA is often subjective and diagnoses frequently differ between pathologists,[23] a pathological diagnosis of AA may not always indicate sameness between gliomas and similar prognosis. However, accurate determination of the pathological group of a tumor is clinically critical for planning adjuvant therapy, such as radiation and chemotherapy. Therefore, genetic analyses, which may reflect causative origins of tumors, are expected to reveal biological traits with less inter-observer variation, as is the case of 1p/19q co-deletion in oligodendroglial tumors. Because *IDH* mutations have a defined role in gliomagenesis and indicate, to some extent, the nature of the original tumor cell, monitoring *IDH* mutational status may allow for accurate assignment of diagnosed AA to low-grade gliomas that frequently harbor *IDH* mutation or to primary GBM that usually have intact *IDH*. Therefore, we believe that monitoring *IDH* mutation in combination with 1p/19q co-deletion, which genetically differentiates oligodendroglial and astrocytic tumors, could be a useful genetic marker of prognostic value, especially for grade 3 glioma patients.

Acknowledgments

We appreciate the technical assistance of Reiko Matsuura (Department of Neurosurgery, University of Tokyo, Tokyo, Japan). This work was supported in part by a Grant-in-Aid for Scientific Research (C) (No. 20591706) to A.M. and a Grant-in-Aid for Young Scientists (B) (No. 22791334) to K.S. from the Japan Society for the Promotion of Science. A.M. was also supported by the Takeda Science Foundation.

Disclosure Statement

The authors have no conflicts of interest.

Abbreviations

2-HG	2-hydroxyglutarate
AA	anaplastic astrocytoma
AOA	anaplastic oligoastrocytoma
AOG	anaplastic oligodendroglioma

DA	diffuse astrocytoma
GBM	glioblastoma
GBMO	glioblastoma with oligodendroglioma component
GGL	ganglioglioma
IDH	isocitrate dehydrogenase
LOH	loss of heterozygosity
MLPA	multiplex ligation-dependent probe amplification
OA	oligoastrocytoma
OG	oligodendroglioma
OS	overall survival
PA	pilocytic astrocytoma
PFS	progression-free survival

References

1 Louis DN, Ohgaki H, Wiestler OD, Cavenee WK, eds. *WHO Classification of Tumours of the Central Nervous System*, 4th edn. Lyon: International Agency for Research on Cancer, 2007.
2 Parsons DW, Jones S, Zhang X *et al.* An Integrated Genomic Analysis of Human Glioblastoma Multiforme. *Science* 2008; **321**: 1807–12.
3 Balss J, Meyer J, Mueller W, Korshunov A, Hartmann C, Deimling A. Analysis of the *IDH1* codon 132 mutation in brain tumors. *Acta Neuropathol (Berl)* 2008; **116**: 597–602.
4 Ichimura K, Pearson DM, Kocialkowski S *et al. IDH1* mutations are present in the majority of common adult gliomas but rare in primary glioblastomas. *Neuro Oncol* 2009; **11**: 341–7.
5 Sonoda Y, Kumabe T, Nakamura T *et al.* Analysis of *IDH1* and *IDH2* mutations in Japanese glioma patients. *Cancer Sci* 2009; **100**: 1996–8.
6 Watanabe T, Nobusawa S, Kleihues P, Ohgaki H. *IDH1* Mutations Are Early Events in the Development of Astrocytomas and Oligodendrogliomas. *Am J Pathol* 2009; **174**: 1149–53.
7 Yan H, Parsons DW, Jin G *et al. IDH1* and *IDH2* mutations in gliomas. *N Engl J Med* 2009; **360**: 765–73.
8 Mardis ER, Ding L, Dooling DJ *et al.* Recurring mutations found by sequencing an acute myeloid leukemia genome. *N Engl J Med* 2009; **361**: 1058–66.
9 Ward PS, Patel J, Wise DR *et al.* The Common Feature of Leukemia-Associated IDH1 and IDH2 Mutations Is a Neomorphic Enzyme Activity Converting α-Ketoglutarate to 2-Hydroxyglutarate. *Cancer Cell* 2010; **17**: 225–34.
10 Bleeker FE, Lamba S, Leenstra S *et al. IDH1* mutations at residue p.R132 ($IDH1^{R132}$) occur frequently in high-grade gliomas but not in other solid tumors. *Hum Mutat* 2009; **30**: 7–11.
11 Dang L, White DW, Gross S *et al.* Cancer-associated IDH1 mutations produce 2-hydroxyglutarate. *Nature* 2009; **462**: 739–44.
12 Xu W, Yang H, Liu Y *et al.* Oncometabolite 2-Hydroxyglutarate Is a Competitive Inhibitor of α-Ketoglutarate-Dependent Dioxygenases. *Cancer Cell* 2011; **19**: 17–30.
13 Lesniak M, Jin G, Reitman ZJ *et al.* 2-Hydroxyglutarate Production, but Not Dominant Negative Function, Is Conferred by Glioma-Derived NADP+-Dependent Isocitrate Dehydrogenase Mutations. *PLoS ONE* 2011; **6**: e16812.
14 Nobusawa S, Watanabe T, Kleihues P, Ohgaki H. *IDH1* Mutations as Molecular Signature and Predictive Factor of Secondary Glioblastomas. *Clin Cancer Res* 2009; **15**: 6002–7.
15 Sanson M, Marie Y, Paris S *et al.* Isocitrate Dehydrogenase 1 Codon 132 Mutation Is an Important Prognostic Biomarker in Gliomas. *J Clin Oncol* 2009; **27**: 4150–4.
16 Van den Bent MJ, Dubbink HJ, Marie Y *et al. IDH1* and *IDH2* Mutations Are Prognostic but not Predictive for Outcome in Anaplastic Oligodendroglial Tumors: a Report of the European Organization for Research and Treatment of Cancer Brain Tumor Group. *Clin Cancer Res* 2010; **16**: 1597–604.
17 Shibahara I, Sonoda Y, Kanamori M *et al. IDH1/2* gene status defines the prognosis and molecular profiles in patients with grade III gliomas. *Int J Clin Oncol* 2011; DOI: 10.1007/s10147-011-0323-2 [Epub ahead of print].
18 Dubbink HJ, Taal W, Van Marion R *et al. IDH1* mutations in low-grade astrocytomas predict survival but not response to temozolomide. *Neurology* 2009; **73**: 1792–5.
19 Houillier C, Wang X, Kaloshi G *et al. IDH1* or *IDH2* mutations predict longer survival and response to temozolomide in low-grade gliomas. *Neurology* 2010; **75**: 1560–6.
20 Kim Y-H, Nobusawa S, Mittelbronn M *et al.* Molecular Classification of Low-Grade Diffuse Gliomas. *Am J Pathol* 2010; **177**: 2708–14.
21 Jha P, Suri V, Sharma V *et al. IDH1* mutations in gliomas: first series from a tertiary care centre in India with comprehensive review of literature. *Exp Mol Pathol* 2011; **91**: 385–93.
22 Qi SA, Yu L, Lu YT *et al. IDH* mutations occur frequently in Chinese glioma patients and predict longer survival but not response to concomitant chemoradiotherapy in anaplastic gliomas. *Oncol Rep* 2011; **26**: 1479–85.
23 Ueki K, Nishikawa R, Nakazato Y *et al.* Correlation of histology and molecular genetic analysis of 1p, 19q, 10q, *TP53*, *EGFR*, *CDK4*, and *CDKN2A* in 91 astrocytic and oligodendroglial tumors. *Clin Cancer Res* 2002; **8**: 196–201.
24 Mukasa A, Ueki K, Matsumoto S *et al.* Distinction in gene expression profiles of oligodendrogliomas with and without allelic loss of 1p. *Oncogene* 2002; **21**: 3961–8.
25 Esteller M, Hamilton SR, Burger PC, Baylin SB, Herman JG. Inactivation of the DNA repair gene O6-methylguanine-DNA methyltransferase by promoter hypermethylation is a common event in primary human neoplasia. *Cancer Res* 1999; **59**: 793–7.
26 Labussiere M, Idbaih A, Wang XW *et al.* All the 1p19q codeleted gliomas are mutated on *IDH1* or *IDH2*. *Neurology* 2010; **74**: 1886–90.
27 Korshunov A, Meyer J, Capper D *et al.* Combined molecular analysis of *BRAF* and *IDH1* distinguishes pilocytic astrocytoma from diffuse astrocytoma. *Acta Neuropathol* 2009; **118**: 401–5.
28 Horbinski C, Kofler J, Yeaney G *et al.* Isocitrate dehydrogenase 1 analysis differentiates gangliogliomas from infiltrative gliomas. *Brain Pathol* 2011; **21**: 564–74.
29 Figueroa ME, Abdel-Wahab O, Lu C *et al.* Leukemic IDH1 and IDH2 Mutations Result in a Hypermethylation Phenotype, Disrupt TET2 Function, and Impair Hematopoietic Differentiation. *Cancer Cell* 2010; **18**: 553–67.
30 Christensen BC, Smith AA, Zheng S *et al.* DNA Methylation, Isocitrate Dehydrogenase Mutation, and Survival in Glioma. *J Natl Cancer Inst* 2010; **103**: 143–53.
31 Laffaire J, Everhard S, Idbaih A *et al.* Methylation profiling identifies 2 groups of gliomas according to their tumorigenesis. *Neuro Oncol* 2010; **13**: 84–98.
32 Noushmehr H, Weisenberger DJ, Diefes K *et al.* Identification of a CpG Island Methylator Phenotype that Defines a Distinct Subgroup of Glioma. *Cancer Cell* 2010; **17**: 510–22.
33 Hegi ME, Diserens AC, Gorlia T *et al. MGMT* gene silencing and benefit from temozolomide in glioblastoma. *N Engl J Med* 2005; **352**: 997–1003.
34 Rivera AL, Pelloski CE, Gilbert MR *et al.* MGMT promoter methylation is predictive of response to radiotherapy and prognostic in the absence of adjuvant alkylating chemotherapy for glioblastoma. *Neuro Oncol* 2010; **12**: 116–21.
35 Van den Bent MJ, Dubbink HJ, Sanson M *et al. MGMT* promoter methylation is prognostic but not predictive for outcome to adjuvant PCV chemotherapy in anaplastic oligodendroglial tumors: a report from EORTC Brain Tumor Group Study 26951. *J Clin Oncol* 2009; **27**: 5881–6.
36 Hartmann C, Hentschel B, Wick W *et al.* Patients with *IDH1* wild type anaplastic astrocytomas exhibit worse prognosis than *IDH1*-mutated glioblastomas, and *IDH1* mutation status accounts for the unfavorable prognostic effect of higher age: implications for classification of gliomas. *Acta Neuropathol (Berl)* 2010; **120**: 707–18.

doi: 10.1111/j.1349-7006.2011.02175.x

J Neurooncol (2011) 103:619–627
DOI 10.1007/s11060-010-0433-0

CLINICAL STUDY – PATIENT STUDY

Prediction of malignancy grading using computed tomography perfusion imaging in nonenhancing supratentorial gliomas

Takaaki Beppu · Makoto Sasaki · Kohsuke Kudo · Akira Kurose · Masaru Takeda · Hiroshi Kashimura · Akira Ogawa · Kuniaki Ogasawara

Received: 10 June 2010 / Accepted: 20 September 2010 / Published online: 15 October 2010

Abstract Tumor grade differentiation is often difficult using routine neuroimaging alone. Computed tomography perfusion imaging (CTP) provides quantitative information on tumor vasculature that closely parallels the degree of tumor malignancy. This study examined whether CTP is useful for preoperatively predicting the grade of malignancy in glioma showing no enhancement on contrast-enhanced magnetic resonance imaging (MRI). Subjects comprised 17 patients with supratentorial glioma without enhancement on MRI. CTP was performed preoperatively, and absolute values and normalized ratios of parameters were calculated. Postoperatively, subjects were classified into two groups according to histological diagnosis of grade 3 (G3) glioma or grade 2 (G2) glioma. Absolute values and normalized ratios for each parameter were compared between G3 and G2. Accuracies of normalized ratios for cerebral blood flow (*n*CBF) and cerebral blood volume (*n*CBV) in predicting a diagnosis of G3 were assessed. In addition, *n*CBV was compared between diffuse astrocytoma, G2 oligodendroglial tumor (OT), and G3 OT. Values for *n*CBF and *n*CBV differed significantly between G3 and G2. Using *n*CBV of 1.6 as a cutoff, specificity and sensitivity for distinguishing G3 were 83.3% and 90.9%, respectively. No significant difference in *n*CBV was seen between diffuse astrocytoma and G2 OT, whereas differences were noted between G2 and G3 OTs, and between diffuse astrocytoma and G3 OT. CTP offers a useful method for differentiating between G3 and G2 in nonenhancing gliomas.

Keywords Computed tomography perfusion imaging · Diffuse astrocytoma · Glioma · Nonenhancement · Oligodendroglioma · Preoperative diagnosis

T. Beppu (✉) · M. Takeda · H. Kashimura · A. Ogawa · K. Ogasawara
Department of Neurosurgery, Iwate Medical University, Uchimaru 19-1, Morioka 020-8505, Japan
e-mail: tbeppu@iwate-med.ac.jp

M. Sasaki · K. Kudo
Advanced Medical Research Center, Iwate Medical University, Morioka, Japan

A. Kurose
Department of Pathology, Iwate Medical University, Morioka, Japan

Introduction

Glioma is graded according to World Health Organization (WHO) classification, with grade 1 or 2 graded as low-grade glioma (LGG) and grade 3 or 4 commonly defined as high-grade glioma (HGG) [1]. As treatment and prognosis differ substantially between LGG and HGG, the ability to differentiate between grade 2 (G2) glioma and grade 3 (G3) glioma, as the border between LGG and HGG, is very important. On contrast-enhanced computed tomography (CT) and magnetic resonance imaging (MRI), G2 gliomas are nonenhanced due to preservation of blood–brain barrier (BBB), whereas G3 gliomas are commonly enhanced due to increased vascular permeability caused by disruption of the BBB within the tumor [2–4]. However, the relationship between histological grading and contrast enhancement on CT and MRI is not always clear. Preoperatively differentiating between G3 and G2 gliomas that are nonenhanced on conventional neuroimaging is often difficult. When patients with nonenhancing glioma are encountered, neurooncologists may perform various examinations to differentiate between G3 and G2 gliomas, such as positron emission tomography (PET) for direct assessment of tumor

metabolism, magnetic resonance spectroscopy to detect magnetic resonance signals of metabolites, and diffusion-weighted MRI to clarify structures within and surrounding the tumor. Assessment of intratumoral vasculature is one approach that may help to clarify the intratumoral biological characteristics and malignancy of a tumor, as intratumoral angiogenesis and high vascularity, which are regulated by hypoxia and various vascular endothelial growth factors, are essential for tumor growth and progression [5–7].

Angiography enables direct observation of intratumoral vessels, but is hazardous and remains limited for depiction of intratumoral microvasculature. Magnetic resonance perfusion imaging (MRP) and CT perfusion imaging (CTP) provide reliable information on the intratumoral microvasculature [8–12]. Numerous studies of perfusion imaging have shown that increasing malignancy of the glioma is associated with increased intratumoral blood volume and vascular permeability [10, 13–15]. Quantitative evaluation from perfusion imaging thus depends on both the microvasculature (vascular density and diameter), and vascular permeability due to disruption or absence of the BBB within the tumor. Previous reports have shown good correlations between findings on perfusion imaging and malignancy grading in enhancing glioma. In contrast, the BBB of vessels is preserved in nonenhancing glioma, since extravasation of contrast medium through the BBB in tumor vessels is considered to represent the main cause of tumor contrast enhancement [4]. As MRI remains the preferred technique for assessing brain tumors, studies using MRP to thoroughly evaluate gliomas greatly outnumber those using CTP, and MRP has also been applied to neurooncological applications for nonenhancing gliomas, such as determining biopsy targets and predicting malignant progression [16–18]. In recent years, CTP has gained acceptance as a valuable imaging technique for assessing hemodynamics in brain tumors [13, 14, 19–22]. However, whether CTP is useful for grading malignancy of nonenhancing gliomas remains unclear. CTP retains the advantage of a linear relationship between attenuation changes on CT and tissue concentration of contrast medium, unlike MRP [8, 20]. We therefore hypothesized that CTP should accurately provide quantitative information on only the microvasculature within the tumor, excluding extravasation due to permeability, when limited to patients with nonenhancing glioma. In the present study, we performed CTP on patients with nonenhancing glioma, and compared cerebral blood volume (CBV), cerebral blood flow (CBF), and mean transit time (MTT), as quantitative values provided from CTP, with postoperative histological diagnosis. The present study aims to determine whether CTP is useful for prediction of preoperative malignancy grading (WHO G2 or G3) in nonenhancing glioma on contrast-enhanced MRI.

Patients and methods

Patients

The study protocol was approved by the Ethics Committee of Iwate Medical University, Morioka, Japan. Consecutive patients admitted to the Department of Neurosurgery at Iwate Medical University between September 2006 and January 2010 and meeting the entry criteria were recruited to this study. Entry criteria for this study comprised: diagnosis of supratentorial glioma; tumor bulk not clearly enhanced on gadolinium-enhanced T1-weighted MRI (Gd-T1WI); tumor bulk sited in the supratentorial cerebrum; no past history relating to the brain, including surgical operation, irradiation, administration of anticancer agents or steroids, stroke, infection, or other disorders such as demyelinating disease; and provision of written informed consent to participate. Subjects comprised 17 patients (7 men, 10 women) with mean age of 47.8 years. Patient data including age, tumor site, operation method, postoperative histological diagnosis, and malignancy grade are summarized in Table 1.

Table 1 Patient summary

No.	Age (years)	Tumor site	Surgery	Histology	WHO grade
1	76	Temporal lobe	Biopsy	AA	3
2	58	Frontal lobe	Resection	AO	3
3	45	Frontal lobe	Resection	AO	3
4	34	Frontal lobe	Resection	AO	3
5	29	Frontal lobe	Resection	AO	3
6	21	Frontal lobe	Resection	AOA	3
7	78	Frontal lobe	Biopsy	DA	2
8	68	Frontal lobe	Biopsy	DA	2
9	68	Parietal lobe	Biopsy	DA	2
10	65	Frontal lobe	Resection	DA	2
11	58	Frontal lobe	Resection	DA	2
12	52	Frontal lobe	Resection	Oli	2
13	46	Temporal lobe	Resection	Oli	2
14	42	Frontal lobe	Resection	OA	2
15	30	Frontal lobe	Resection	OA	2
16	27	Frontal lobe	Resection	DA	2
17	16	Temporal lobe	Resection	OA	2

AA anaplastic astrocytoma, *AO* anaplastic oligodendroglioma, *AOA* anaplastic oligoastrocytoma, *DA* diffuse astrocytoma, *Oli* oligodendroglioma, *OA* oligoastrocytoma

Conventional MRI and CTP

Conventional MRI was performed for all subjects within 7 days before surgery. Spin-echo Gd-T1WI was performed approximately 2 min after intravenous injection of gadolinium (0.2 ml/kg, Magnevist; Bayer Schering Pharma, Berlin, Germany), using a 3.0-T whole-body scanner (GE Yokogawa Medical Systems, Tokyo, Japan) with a standard head coil. We confirmed that the tumor in each patient did not show clear enhancement with gadolinium on Gd-T1WI.

CTP was also performed within 7 days before surgery using a 16-row multidetector CT system (Aquillion 16; Toshiba Medical Systems, Tokyo, Japan), in accordance with the methods described by Sasaki et al. [23]. After performing noncontrast CT to determine the location of the tumor balk, a multislice scan targeting the tumor bulk was performed (80 kV_p; 40 mA; 1.5 s/rotation, 30 rotations field of view, 240 × 240 mm^2; four contiguous 8-mm-thick sections; total scan time, 45 s). Five seconds after intravenously injecting 40 ml (4 ml/s) nonionic iodine contrast medium (Iopamiron 300; Bayer Schering Pharma) using a power injector, dynamic scanning was started and tissue attenuation of contrast medium was monitored on a slice. Radiation doses for the scanning protocol were as follows: volume CT dose index, 150 mGy; dose–length product, 480 mGy cm; and effective dose, 1.34 mSv. Data were transferred to a commercial workstation (M900 Quadra; Ziosoft, Tokyo, Japan), and scaled color maps for CBF, CBV, and MTT were automatically created. All mathematical analyses were performed by the deconvolution method [19, 24], using CTP analysis software supplied with the workstation described above. Among the three types of deconvolution algorithms implemented in this software, we used the block-circulant singular value decomposition method. Regions of interest (ROI) for venous output and arterial input functions were manually placed at the superior sagittal sinus and a single branch of the insular segment of the middle cerebral artery on either the pathological or nonpathological side, or A2 segment of the anterior cerebral artery, respectively. ROI were also placed over the entire tumor bulk and apparently normal white matter (ANWM) on the nonpathological side, on color maps for each parameter. Size of the ROI for ANWM was established as 1.0 cm^2. In the measurement of absolute values, the vascular-pixel elimination (VPE) method was used to exclude pixels from large vessels at the cerebral surface, sulci, and cisterns [23, 25]. In the present study, we established the VPE threshold as 6.0 ml/100 g for CBV, since high-CBV areas suggesting large cortical vessels on color map disappeared satisfactorily at 6.0 ml/100 g when the threshold was varied between 5.0 and 8.0 ml/100 g using our analysis software. Large vascular pixels were thus defined as pixels with CBV values >6.0 ml/100 g and were automatically eliminated. Regional absolute values (*r*CBF, *r*CBV, and *r*MTT) were then calculated automatically for all ROI. The measurements described above were performed twice for each patient by two investigators (M.S. and K.K.) who were blinded to all clinical data, including individual patient information and histological diagnosis. Absolute values of all parameters for each patient were determined as the mean of four measured values, as determined twice by each investigator. The second test was performed 1 week after the first test, with a different randomized order of measurements from the first test. We also calculated normalized ratios (*n*CBF, *n*CBV, and *n*MTT) as the absolute value for the tumor divided by the absolute value for the ANWM for each parameter in all patients. All patients underwent surgery, with tumor resection for 13 patients and CT-guided stereotactic needle biopsy for 4 patients (Table 1). The region targeted in stereotactic biopsy was based on findings from the CBV color map. If the color map showed heterogeneous perfusion within the tumor, the targeted region corresponded to the region with the highest perfusion area for CBV. In cases with tumor resection, histological diagnosis was determined by observation at the lesion showing the most malignant histological features in all preparations. Postoperatively, histological diagnosis using specimens obtained from surgery was made by one of the investigators (A.K.) with no prior knowledge of CTP data.

Statistical analyses

All data were analyzed using PASW Statistics version 18 software (SPSS Japan, Tokyo, Japan). Inter- and intrarater reliabilities for all absolute values were evaluated according to classification of the intraclass correlation coefficient (ICC) [26]. For $ICC_{(1,1)}$ and $ICC_{(1,k)}$ as interrater reliability, agreement of all absolute values (CBF, CBV, and MTT) between first and second tests was analyzed for tumor and ANWM for each investigator, using one-factor analysis of variance (ANOVA). For $ICC_{(2,1)}$ and $ICC_{(2,k)}$ as intrarater reliability, agreement of all absolute values between the two investigators was analyzed for tumor and ANWM for each test, using two-factor ANOVA. Patients were assigned to one of two histological grading groups according to histological classification: WHO G2 or WHO G3. Frequency of biopsy was compared between G2 and G3 groups using Fisher's exact probability test. We compared absolute values from the tumor lesion for each parameter between G2 and G3 using the Mann–Whitney *U* test. Furthermore, the normalized ratio for each parameter was compared between these groups again using the Mann–Whitney *U* test. The accuracy of *r*CBF and *n*CBV in predicting a diagnosis of G3 was assessed using receiver

operating characteristic (ROC) curves. ROC curves were calculated in increments of 0.1. Absolute values and normalized ratios for CBV were compared between diffuse astrocytoma, G2 oligodendroglial tumor (OT), and G3 OT, using the Mann–Whitney U test. G2 OTs comprised oligodendroglioma or oligoastrocytoma, whereas G3 OTs comprised anaplastic oligodendroglioma or anaplastic oligoastrocytoma. Statistical significance was established at the $P < 0.05$ level in all analyses.

Results

Based on histological diagnosis after surgery, 6 patients were assigned to the G3 group and 11 patients were assigned to the G2 group (Table 1). Of these 17 patients, 4 patients underwent stereotactic biopsy. Frequency of biopsy did not differ significantly between G3 and G2 groups ($P = 0.25$).

Interrater reliability was classified as "almost perfect" for both tumor and ANWM for each investigator: $ICC_{(1,1)}$ and $ICC_{(1,k)}$ for M.S. were 0.943 and 0.971 for tumor, and 0.961 and 0.980 for ANWM, respectively, and those for K.K. were 0.966 and 0.983 for tumor, and 0.942 and 0.970 for ANWM, respectively. Intrarater reliability was also classified as "almost perfect" for both tumor and ANWM in each test: $ICC_{(2,1)}$ and $ICC_{(2,k)}$ in the first test were 0.987 and 0.993 for tumor, and 0.973 and 0.987 for ANWM, respectively, and those in the second test were 0.971 and 0.985 for tumor, and 0.973 and 0.986 for ANWM, respectively. Absolute values of tumor lesions for each parameter in G3 and G2 groups are summarized in Table 2. Absolute values for all parameters varied widely, with no significant differences in any parameters identified between G3 and G2 groups. Normalized ratios for each parameter are summarized in Table 3. Significant differences between G3 and G2 groups were identified for nCBF and nCBV, with no significant differences in nMTT.

The cutoff for accuracy was defined as the point lying closest to the upper-left corner of the ROC curve.

Table 2 Absolute values for each parameter

	rCBF (ml/100 g/min)	rCBV (ml/100 g)	rMTT (s)
G3 ($n = 6$)			
Range	10.8–27.0	1.9–3.2	6.8–10.8
Mean ± SD	18.3 ± 5.3	2.5 ± 0.5	8.5 ± 1.5
G2 ($n = 11$)			
Range	8.8–23.3	1.3–2.6	7.0–12.2
Mean ± SD	15.5 ± 4.2	2.1 ± 0.4	8.8 ± 1.5
P	0.27	0.25	0.76

SD standard deviation

Table 3 Normalized ratios for each parameter

	nCBF	nCBV	nMTT
G3 ($n = 6$)			
Range	1.34–3.00	1.54–2.39	0.76–1.06
Mean ± SD	2.10 ± 0.57	1.92 ± 0.37	0.90 ± 0.12
G2 ($n = 11$)			
Range	0.92–2.00	0.91–1.75	0.79–1.07
Mean ± SD	1.41 ± 0.38	1.26 ± 0.28	0.91 ± 0.09
P	0.01	0.004	0.76

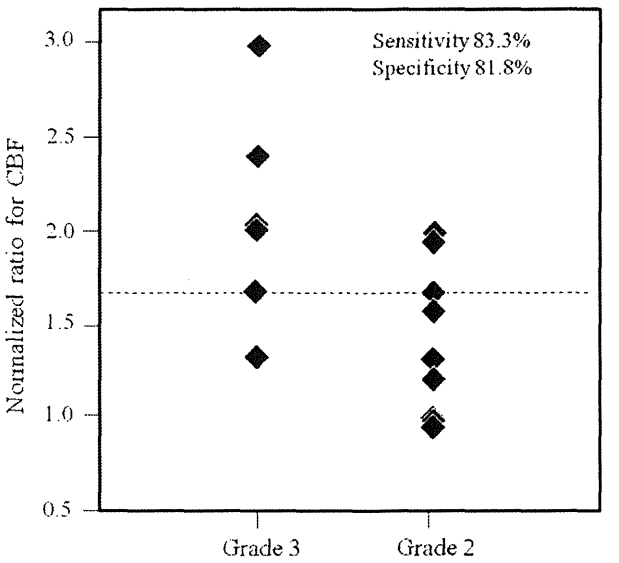

Fig. 1 Relationship between nCBF value and WHO grading. Using a cutoff of 1.7 (*dashed line*), nCBV was ≥1.7 for 5 (83.3%) of 6 patients with G3, compared with <1.7 for 9 (63.6%) of 11 patients with G2

Sensitivity and specificity in predicting a diagnosis of G3 were 83.3% and 81.8% for nCBF (cutoff 1.7), and 83.3% and 90.9% for nCBV (cutoff 1.6) (Figs. 1, 2). Accuracy for predicting a diagnosis of G3 was higher with nCBV than with nCBF.

A comparison of nCBV was made between G3 OT, G2 OT, and diffuse astrocytoma (Table 4). Significant differences in nCBV were identified between G3 and G2 OTs ($P = 0.009$), and between G3 OT and diffuse astrocytoma ($P = 0.02$), whereas no significant difference was seen between G2 OT and diffuse astrocytoma ($P = 0.36$).

Illustrative cases

We now describe the cases of two patients for whom CTP provided useful information for predicting tumor grading. Gd-T1WI for case 6 showed glioma with no clear enhancement in the right frontal lobe (Fig. 3a). Using the

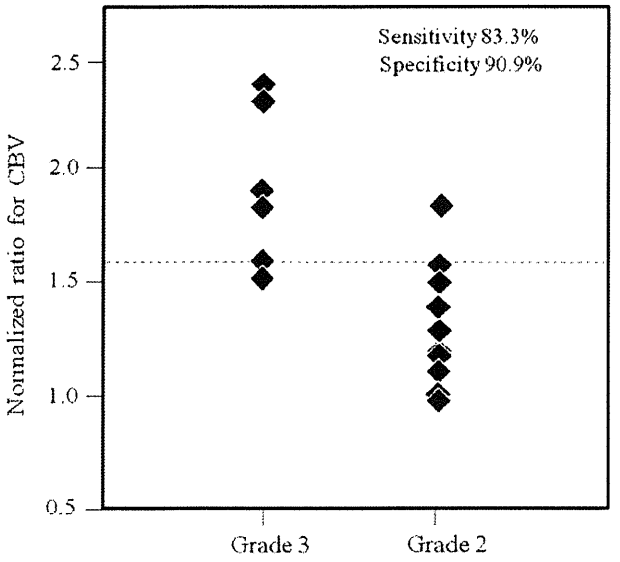

Fig. 2 Relationship between *n*CBV value and WHO grading. Using a cutoff point of 1.6 (*dashed line*), *n*CBV was ≥1.6 for 5 (83.3%) of 6 patients with G3 and <1.6 for 10 (90.9%) of 11 patients with G2

Table 4 Normalized ratio (mean ± SD) for CBV in G3 OT, G2 OT, and diffuse astrocytoma

	*n*CBV
G3 OT ($n = 5$)	1.99 ± 0.36
G2 OT ($n = 5$)	1.16 ± 0.24
Diffuse astrocytoma ($n = 6$)	1.35 ± 0.31

OT oligodendroglial tumors

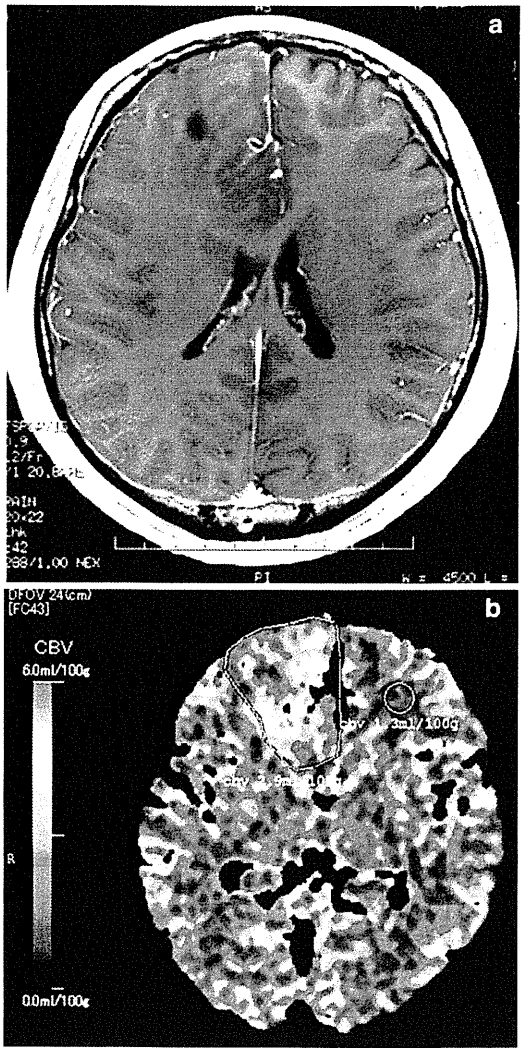

Fig. 3 Gd-T1WI (**a**) and color map of CBV (**b**) for case 6. *Circle* ROI covering the entire tumor bulk and ANWM localized on the nonpathological side

VPE method, color mapping of CBV demonstrated large vessels of the cerebral surface to be successfully excluded (Fig. 3b). Color mapping of CBV depicted areas of hyperperfusion within the tumor. The *n*CBV for this case (*n*CBV = 2.3) was higher than the cutoff point. Tissue specimens obtained from gross total resection showed typical histological features of G3 anaplastic oligoastrocytoma.

Gd-T1WI for case 14 showed nonenhancing glioma of the right frontal lobe (Fig. 4a). The VPE method satisfactorily eliminated large vessels of the cerebral surface (Fig. 4b). On color mapping, areas of hyperperfusion seemed to be minor compared with those in case 6. The *n*CBV in this case (*n*CBV = 1.2) was lower than the cutoff point. After tumor resection, histological diagnosis was G2 oligoastrocytoma.

Discussion

Previous reports have documented that G3 gliomas make up 40–46% of nonenhancing gliomas on conventional MRI [3, 4]. Our finding of G3 tumors in 6 (35.2%) of 17 patients was close to this level. Thus, preoperative differentiation between G3 and G2 using MRI is often difficult. Biopsy or resection allowing histological diagnosis currently remain the basis for differentiation between G3 and G2 gliomas. However, neuroimaging can provide useful information on pathological diagnosis, particularly for patients who do not undergo biopsy or resection allowing histological diagnosis. Novel neuroimaging procedures other than routine MRI are thus desired. CTP and MRP provide reliable information on tumor vasculature, which can help to determine the extent of malignancy in glioma [8, 10, 22]. Although limitations of CTP include radiation dose and limited area of coverage compared with MRP, the linear relationship between attenuation changes on CT and tissue concentration of contrast medium and the lack of confounding sensitivity to flow artifacts allow CTP to

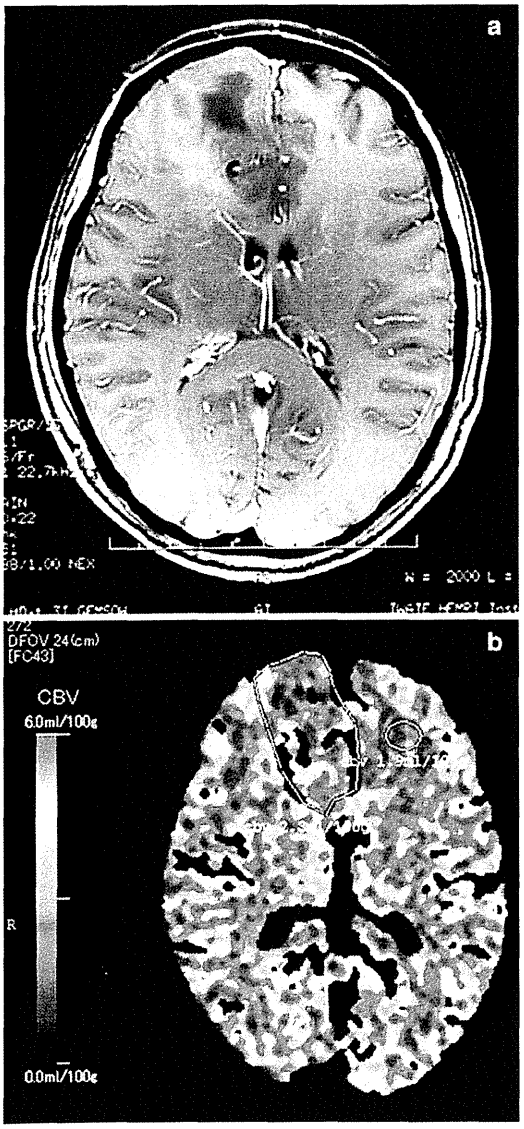

Fig. 4 Gd-T1WI (**a**) and color map of CBV (**b**) for case 14. *Circle* ROI covering the entire tumor bulk and ANWM localized on the nonpathological side

potentially offer a more accurate representation of tissue microvasculature than similar MRP studies [8, 20]. Furthermore, CTP offers advantages such as measurement of quantitative absolute values, greater availability, fast scanning time, high spatial resolution, low cost, and the ability to use this technique for patients who cannot undergo MRI due to the presence of metallic materials in the body [14, 22, 27].

CBF derived from CTP has been suggested to show a tendency toward overestimation, compared with that derived from PET [28]. Since overestimation of CBF in CTP was attributable to the presence of large vessels on the cerebral surface, as contrast materials act as a nondiffusible intravascular tracer in CTP unlike in PET, the VPE method has been proposed to eliminate flow in large vessels [25]. Accurate measurement of CBV contributes to accurate CBF and MTT, as these parameters are closely associated in the central volume principle as CBF = CBV/MTT [29]. We therefore used the VPE method in the present study. We think that optimal threshold differs according to the specific analysis software used for CTP. While VPE threshold was 8.0 ml/100 g in the report by Kudo et al. [25], we established a threshold of 6.0 ml/100 g, since high-CBV areas from cortical large vessels disappeared satisfactorily at this threshold for the analysis software used in our study. Another reason for using the VPE method is that OTs are commonly seen as superficially located tumors in the brain [30, 31]. Elimination of superficial large vessels at the cerebral surface, sulci, and cisterns thus seems warranted when CTP is performed for OTs.

In previous reports of CTP, *r*CBV values ranged from 2.3 to 8.87 ml/100 g for HGG and from 0.95 to 3.28 ml/100 g for LGG, differing significantly between HGG and LGG [13, 14, 20]. The present mean rCBV values in G3 and G2 (Table 2) agreed with previous findings. In addition, mean rCBV values in both G3 and G2 were less than half of 6.0 ml/100 g as VPE threshold. These findings suggest that the VPE method used in this study did not exclude tumor vessels along with other large vessels from CBV maps. While *r*CBV for G3 tended to be on the low side compared with previous reports, this could have resulted from the exclusion of patients with enhancing glioma as subjects in this study. Extravasation of contrast medium through the BBB in enhanced glioma may directly lead to increased CBV, due to the linear relationship between attenuation changes on CT and tissue concentration of contrast medium. Jain et al. [20] documented that *r*CBF and *r*CBV in nonenhancing G3 glioma do not differ significantly from those in nonenhancing G2 glioma, although sample size in that report was small. The present study with more subjects suggested that even nonenhancing G3 glioma retains more vascular density than G2, although the difference in *r*CBV between the two groups was minor (Table 2). However, this result might have been influenced by the disproportionate number of OTs in the G2 (42%) and G3 (83%) groups. If vascular density is significantly higher in G3 OT than in anaplastic astrocytoma, the large number of G3 OTs may have result in a high mean CBV for the G3 group in this study. This issue represents a definite limitation to the present study.

Concentration of contrast medium within the tumor might be subtly influenced by individual parameters such as body size and cardiac output volume, and differences in analytical software among institutes. We must emphasize the importance of estimation using normalized ratios, as

this allows us to ignore these differences. Ellika et al. [22] reported findings for *n*CBV using CTP in 19 patients with glioma, composed of a mixture of enhancing and nonenhancing WHO G1–G4 gliomas, and the utility of *n*CBF and *n*CBV for distinguishing HGG from LGG. They also documented *n*CBF and *n*CBV ranges of 0.78–3.75 and 1.5–3.7 in two patients with nonenhancing G3 glioma, and ranges of 1.26–1.48 and 0.94–1.72 in three patients with nonenhancing G2 glioma, respectively. Mean values of *n*CBF and *n*CBV in G3 and G2 in this study (Table 3) seemed close to the values reported by Ellika et al.

Radiographic grading of gliomas with conventional MRI is not always accurate, with 85.7% sensitivity for predicting HGG, even when including subjects with enhancing glioma [22]. When subjects are limited to those with nonenhancing gliomas, radiographic grading using conventional MRI should be more difficult. A previous report documented 85.7% sensitivity and 100% specificity for identifying HGG using *n*CBV [22]. In the present study, CTP could distinguish nonenhancing G3 glioma from nonenhancing G2 glioma with 83.3% sensitivity and 90.9% specificity using *n*CBV (Fig. 2). This was superior to the results for *n*CBF. Accuracy for distinguishing G3 using *n*CBV in the present study was by no means inferior to that reported by Ellika et al. [22], but subjects in this study were limited to those with nonenhancing glioma. These results suggest that *n*CBV in CTP is useful as an auxiliary examination in addition to routine neuroimaging for predicting the grade of malignancy in nonenhancing gliomas.

Previous studies using MRP have documented higher relative CBV in OT than in other gliomas [32–34]. Lev et al. [33] suggested that OTs tend to appear as high blood volume lesion on MRP, without respect to tumor grade. Two reports using MRP documented that G2 OTs show higher relative CBV than diffuse astrocytoma [32, 34]. Also in a report using CTP by Narang et al. [15], G2 OTs showed a trend towards higher CBV than G2 astrocytic tumors, although no significant difference was found, and no significant difference in CBV between G3 OTs and G2 OTs was identified. Those reports explained the high relative CBV of OT by a hypothesis based on the specific histological features of fine capillary networks [33]. Furthermore, those reports suggested that grading malignancy may be difficult when patients with OT are included, due to a high relative CBV. In the present study, no significant difference in *n*CBV was seen between diffuse astrocytoma and G2 OT, whereas significant differences were found between G3 OT and G2 OT. The difference between the reports described above and the present investigation might be explained by differences between MRP and CTP, and by the use of the VPE method in this study. Signal changes in dynamic susceptibility contrast (DSC) MRI for MRP do not depend on only the concentration of contrast material, but also on T2* or T2 relaxation rates, which are affected by calcified foci and hemorrhage within tumor tissue. These histological features are commonly seen in OTs. DSC signals might thus be higher in OTs than in diffuse astrocytoma, even when the microvascular densities are comparable. The VPE method may have eliminated pixels of high-CBV vessels in OTs, if vascular density in OTs is significantly higher than that in diffuse astrocytoma. However, exclusion of large vessels at the cerebral surface and sulci from CTP maps is important, as OTs grow superficially in the brain. Cha et al. [32] explained for reason of high relative CBV for OTs in MRP by the predominant cortical location in addition to distinct vascular pattern in OTs. We think that CTP with the VPE method is useful for simple malignancy grading in subjects with OTs. Conversely, MRP offers potential advantages for the diagnosis of OTs. However, CTP should not be performed additionally to MRP if the purpose in examination is achieved by MRP, as CTP retains drawbacks such as radiation dose and iodine contrast medium.

The present study possesses some limitations regarding the interpretation of study results. First, the number of patients in this study was small, with remarkably fewer cases of anaplastic astrocytoma compared with OT in G3, as mentioned above. Further investigation including a larger number of cases of anaplastic astrocytoma is needed. A second limitation is the possible discrepancy between histological diagnosis and the region of highest CBV within the tumor. The region targeted for stereotactic biopsy was not rigorously transferred from the region of highest *r*CBV ("hot spots"). However, risk of histological misdiagnosis caused by sampling error during biopsy might be negligible, since the number of patients who underwent biopsy was small in both G3 and G2, and no significant difference in frequency of biopsy was seen between groups. In patients who underwent tumor resection, histological diagnosis was not made using tissue specimens rigorously corresponding to "hot spots." However, histological diagnosis based on the most malignant histological features should be closely associated with high CBV, as increased malignancy is associated with higher vascular density. CTP with a 16-row multidetector CT scanner, covering only four contiguous 8-mm-thick sections, did not cover the entire tumor bulk in some patients. For those patients, histological diagnosis was made using tumor tissues corresponding to the area depicted in CTP. A third limitation was that data calculated from CTP in this study were not the highest CBV values for a small ROI placed in "hot spots" on a color map, but rather were mean values for a large ROI covering the entire tumor bulk. This issue also influences the second limitation. We thought that the simple protocol in this study, combining absolute values as a mean in a large ROI with histological diagnosis from the

area of the most malignant features, is suitable for application in clinical practice, as tissue sampling error of regions corresponding to a small ROI can be avoided. High ICC in inter- and intrarater reliabilities showed that the protocol used in this study offers high reproducibility.

Conclusions

We performed CTP combined with the VPE method for 17 patients, to clarify whether CTP can accurately differentiate between G3 and G2 nonenhancing glioma. Our results showed that *n*CBV from CTP was highly accurate in differentiating G3 from G2 nonenhancing gliomas. The most important result was that CTP enabled differentiation between G3 and G2 nonenhancing OTs. CTP combined with the VPE method offers a useful technique for differentiating between G3 and G2 in nonenhancing gliomas.

Acknowledgments This study was supported in part by a Grant-in-Aid for Advanced Medical Science Research from the Ministry of Science, Education, Sports, and Culture, Japan.

References

1. Louis DN, Ohgaki H, Wiestler OD, Cavenee WK, Burger PC, Jouvet A, Scheithauer BW, Kleihues P (2007) The 2007 WHO classification of tumours of the central nervous system. Acta Neuropathol 114:97–109
2. Dean BL, Drayer BP, Bird CR, Flom RA, Hodak JA, Coons SW, Carey RG (1990) Gliomas: classification with MR imaging. Radiology 174:411–415
3. Ginsberg LE, Fuller GN, Hashmi M, Leeds NE, Schomer DF (1998) The significance of lack of MR contrast enhancement of supratentorial brain tumors in adults: histopathological evaluation of a series. Surg Neurol 49:436–440
4. Mihara F, Numaguchi Y, Rothman M, Kristt D, Fiandaca M, Swallow L (1995) Non-enhancing supratentorial malignant astrocytomas: MR features and possible mechanisms. Radiat Med 13:11–17
5. Jain RK, Gerlowski LE (1986) Extravascular transport in normal and tumor tissues. Crit Rev Oncol Hematol 5:115–170
6. Shweiki D, Itin A, Soffer D, Keshet E (1992) Vascular endothelial growth factor induced by hypoxia may mediate hypoxia-initiated angiogenesis. Nature 359:843–845
7. Vajkoczy P, Menger MD (2000) Vascular microenvironment in gliomas. J Neurooncol 50:99–108
8. Barnett G (2006) High-grade gliomas. Humana, Totowa
9. Law M, Cha S, Knopp EA, Johnson G, Arnett J, Litt AW (2002) High-grade gliomas and solitary metastases: differentiation by using perfusion and proton spectroscopic MR imaging. Radiology 222:715–721
10. Law M, Yang S, Wang H, Babb JS, Johnson G, Cha S, Knopp EA, Zagzag D (2003) Glioma grading: sensitivity, specificity, and predictive values of perfusion MR imaging and proton MR spectroscopic imaging compared with conventional MR imaging. Am J Neuroradiol 24:1989–1998
11. Eastwood JD, Lev MH, Provenzale JM (2003) Perfusion CT with iodinated contrast material. Am J Roentgenol 180:3–12
12. Hoeffner EG, Case I, Jain R, Gujar SK, Shah GV, Deveikis JP, Carlos RC, Thompson BG, Harrigan MR, Mukherji SK (2004) Cerebral perfusion CT: technique and clinical applications. Radiology 231:632–644
13. Ding B, Ling HW, Chen KM, Jiang H, Zhu YB (2006) Comparison of cerebral blood volume and permeability in preoperative grading of intracranial glioma using CT perfusion imaging. Neuroradiology 48:773–781
14. Eastwood JD, Provenzale JM (2003) Cerebral blood flow, blood volume, and vascular permeability of cerebral glioma assessed with dynamic CT perfusion imaging. Neuroradiology 45:373–376
15. Narang J, Jain R, Scarpace L, Saksena S, Schultz LR, Rock JP, Rosenblum M, Patel SC, Mikkelsen T (2010) Tumor vascular leakiness and blood volume estimates in oligodendrogliomas using perfusion CT: an analysis of perfusion parameters helping further characterize genetic subtypes as well as differentiate from astroglial tumors. J Neurooncol. doi:10.1007/s11060-010-0317-3
16. Maia AC Jr, Malheiros SM, da Rocha AJ, Stavale JN, Guimaraes IF, Borges LR, Santos AJ, da Silva CJ, de Melo JG, Lanzoni OP, Gabbai AA, Ferraz FA (2004) Stereotactic biopsy guidance in adults with supratentorial nonenhancing gliomas: role of perfusion-weighted magnetic resonance imaging. J Neurosurg 101:970–976
17. Danchaivijitr N, Waldman AD, Tozer DJ, Benton CE, Brasil Caseiras G, Tofts PS, Rees JH, Jager HR (2008) Low-grade gliomas: do changes in rCBV measurements at longitudinal perfusion-weighted MR imaging predict malignant transformation? Radiology 247:170–178
18. Price SJ (2010) Advances in imaging low-grade gliomas. Adv Tech Stand Neurosurg 35:1–34
19. Nabavi DG, Cenic A, Craen RA, Gelb AW, Bennett JD, Kozak R, Lee TY (1999) CT assessment of cerebral perfusion: experimental validation and initial clinical experience. Radiology 213: 141–149
20. Jain R, Ellika SK, Scarpace L, Schultz LR, Rock JP, Gutierrez J, Patel SC, Ewing J, Mikkelsen T (2008) Quantitative estimation of permeability surface-area product in astroglial brain tumors using perfusion CT and correlation with histopathologic grade. Am J Neuroradiol 29:694–700
21. Jain R, Scarpace L, Ellika S, Schultz LR, Rock JP, Rosenblum ML, Patel SC, Lee TY, Mikkelsen T (2007) First-pass perfusion computed tomography: initial experience in differentiating recurrent brain tumors from radiation effects and radiation necrosis. Neurosurgery 61:778–786
22. Ellika SK, Jain R, Patel SC, Scarpace L, Schultz LR, Rock JP, Mikkelsen T (2007) Role of perfusion CT in glioma grading and comparison with conventional MR imaging features. Am J Neuroradiol 28:1981–1987
23. Sasaki M, Kudo K, Ogasawara K, Fujiwara S (2009) Tracer delay-insensitive algorithm can improve reliability of CT perfusion imaging for cerebrovascular steno-occlusive disease: comparison with quantitative single-photon emission CT. Am J Neuroradiol 30:188–193
24. Wintermark M, Maeder P, Thiran JP, Schnyder P, Meuli R (2001) Quantitative assessment of regional cerebral blood flows by perfusion CT studies at low injection rates: a critical review of the underlying theoretical models. Eur Radiol 11:1220–1230
25. Kudo K, Terae S, Katoh C, Oka M, Shiga T, Tamaki N, Miyasaka K (2003) Quantitative cerebral blood flow measurement with dynamic perfusion CT using the vascular-pixel elimination method: comparison with H2(15)O positron emission tomography. Am J Neuroradiol 24:419–426
26. Shrout PE, Fleiss JL (1979) Intraclass correlations: uses in assessing rater reliability. Psychol Bull 86:420–428
27. Miles KA, Charnsangavej C, Lee FT, Fishman EK, Horton K, Lee TY (2000) Application of CT in the investigation of angiogenesis in oncology. Acad Radiol 7:840–850

28. Gillard JH, Minhas PS, Hayball MP, Bearcroft PW, Antoun NM, Freer CE, Mathews JC, Miles KA, Pickard JD (2000) Assessment of quantitative computed tomographic cerebral perfusion imaging with H2(15)O positron emission tomography. Neurol Res 22: 457–464
29. Meier P, Zierler KL (1954) On the theory of the indicator-dilution method for measurement of blood flow and volume. J Appl Physiol 6:731–744
30. Piepmeier J, Baehring JM (2004) Surgical resection for patients with benign primary brain tumors and low grade gliomas. J Neurooncol 69:55–65
31. Beppu T, Inoue T, Nishimoto H, Ogasawara K, Ogawa A, Sasaki M (2007) Preoperative imaging of superficially located glioma resection using short inversion-time inversion recovery images in high-field magnetic resonance imaging. Clin Neurol Neurosurg 109:327–334
32. Cha S, Tihan T, Crawford F, Fischbein NJ, Chang S, Bollen A, Nelson SJ, Prados M, Berger MS, Dillon WP (2005) Differentiation of low-grade oligodendrogliomas from low-grade astrocytomas by using quantitative blood-volume measurements derived from dynamic susceptibility contrast-enhanced MR imaging. Am J Neuroradiol 26:266–273
33. Lev MH, Ozsunar Y, Henson JW, Rasheed AA, Barest GD, Harsh GR IV, Fitzek MM, Chiocca EA, Rabinov JD, Csavoy AN, Rosen BR, Hochberg FH, Schaefer PW, Gonzalez RG (2004) Glial tumor grading and outcome prediction using dynamic spin-echo MR susceptibility mapping compared with conventional contrast-enhanced MR: confounding effect of elevated rCBV of oligodendrogliomas. Am J Neuroradiol 25:214–221
34. Maia AC Jr, Malheiros SM, da Rocha AJ, da Silva CJ, Gabbai AA, Ferraz FA, Stavale JN (2005) MR cerebral blood volume maps correlated with vascular endothelial growth factor expression and tumor grade in nonenhancing gliomas. Am J Neuroradiol 26:777–783

ORIGINAL ARTICLE

Neurol Med Chir (Tokyo) 52, 577 ~ 586, 2012

Patterns of Intracranial Glioblastoma Recurrence After Aggressive Surgical Resection and Adjuvant Management: Retrospective Analysis of 43 Cases

Yoshiyuki KONISHI,[1] Yoshihiro MURAGAKI,[1,2] Hiroshi ISEKI,[1,2] Norio MITSUHASHI,[3] and Yoshikazu OKADA[2]

[1]*Faculty of Advanced Techno-Surgery, Institute of Advanced Biomedical Engineering and Science, and Departments of* [2]*Neurosurgery and* [3]*Radiation Oncology, Tokyo Women's Medical University, Tokyo*

Abstract

The present retrospective study evaluated the recurrence patterns after aggressive surgical removal of intracranial glioblastomas in 43 consecutive adult patients. The resection rate of the enhanced lesion on magnetic resonance imaging was 100% and 95–99% in 22 and 21 cases, respectively. All patients received postoperative fractionated radiotherapy (60 Gy in 30 fractions) with additional chemotherapy (25 cases) or vaccine therapy (18 cases). During follow-up (median 17 months), tumor recurrence was identified in 33 patients, most frequently regional within the wall of the resection cavity (20 cases). No clinical factor differed significantly between the groups of patients with regional or marginal tumor progression (N = 22) and patients with distant or multiple recurrences (N = 8). Progression-free survival did not differ significantly between these two groups (p = 0.27). However, overall survival was significantly longer (p = 0.04) in patients with regional or marginal tumor progression, and constituted 90% and 54% at 1 and 2 years after surgery, respectively, compared to 75% and 0% in patients with distant or multiple recurrences. Aggressive surgical resection and adjuvant management of intracranial glioblastoma may change its recurrence pattern. Tumor progression appears in the wall of the resection cavity or within 2 cm from its margin in approximately half of patients.

Key words: glioblastoma, gross total resection, progression, recurrence, survival

Introduction

Glioblastoma is the most common primary brain tumor in adults and carries an extremely grim prognosis. Management usually includes surgical resection followed by postoperative fractionated radiotherapy (FRT) as well as concomitant and adjuvant chemotherapy. Nevertheless, the incidences of recurrence, regrowth, and dissemination of the tumor are very high due to the well-known infiltrative extension far beyond the boundaries of the localized lesion identifiable with neuroimaging.[4,20,33,37,48] The progression of glioblastoma after treatment in up to 97% of cases occurs either from the bulk of the mass or within 20 mm from the border of its enhanced part identifiable on T_1-weighted magnetic resonance (MR) imaging, and the presence of such local recurrence may be associated with impaired prognosis.[2,3,12,13,23,25,32,34,35,43,44,54] Therefore, various methods for improvement of tumor control at the time of both initial and salvage treatment have been proposed, such as inclusion of the marginal brain tissue in the high dose area during FRT,[4,17,20,26,31–33,35,49,50] additional dose boost with stereotactic radiosurgery,[14,18,41] brachytherapy,[10,36,43] implantation of Gliadel wafers (Guilford Pharmaceuticals Inc., Baltimore, Maryland, USA),[53] or various types of intralesional immunotherapy.[7,42]

The majority of studies on progression of intracranial gliomas after initial treatment have included many cases with incomplete surgical tumor removal. Contemporary advances in neurosurgical technique and introduction of modern intraoperative technologies now permit attain gross total resection of the brain tumor in many cases.[16,19,24,28,30,39,45] Surgical treatment in the vast majority of gliomas could not be considered as curative, but more complete removal of the localized part of the neoplasm may change the dynamics of further growth and

Received November 28, 2011; Accepted February 27, 2012

related prognosis.[11,31]

The present retrospective analysis tried to evaluate the recurrence patterns of intracranial glioblastomas after aggressive surgery.

Materials and Methods

This retrospective study was initiated in September 2009. There were two initial selection criteria: surgery for newly diagnosed glioma performed in the intelligent operating theater of Tokyo Women's Medical University with the use of intraoperative MR (iMR) imaging; and final histopathological diagnosis of glioblastoma. Retrospective backward selection of cases from the constantly maintained computer database was started from June 2008 to allow a minimum of 12-month follow up after completion of postoperative FRT in surviving patients. Case selection was limited to the beginning of 2004, since the initial period after installation of iMR imaging in our clinic (2000) was completed by this time, significant improvement of the intraoperative image quality had succeeded, and the surgical algorithm of glioma treatment in this facility was fully established.[16,27,28,30] All selected cases were checked for resection rate. The established cut-off level of 95% or greater tumor removal was chosen, because this value corresponds to the grading of resection of malignant gliomas used by The Committee of Brain Tumor Registry of Japan.[5]

A total of 65 consecutive patients underwent craniotomy and removal of the newly diagnosed intracranial glioblastoma in the intelligent operating theater of the Tokyo Women's Medical University from January 2004 to June 2008. Resection of 95% or greater was attained in 47 patients. Four patients from this cohort were excluded from further analysis due to omission of postoperative FRT. The remaining 43 patients were included in the present study. The 29 men and 14 women were aged from 18 to 79 years (median 43 years). Eighteen patients were less than 50 years old. Karnofsky performance scale (KPS) score before surgery was 100–80 in 31 patients, 70–60 in 6, and 50 or less in 6. The tumor was predominantly located within the frontal (19 cases), temporal (12 cases), parietal (7 cases), and occipital (3 cases) lobes. Other locations were encountered in only 2 patients. The left hemisphere was affected slightly more often than right (23 vs. 20 cases). According to recursive partitioning analysis classification[6] 12 patients had class III, 21 had class IV, and 10 had class V.

Tumor removal was performed according to our concept of information-guided surgery[17,28,30] with the use of iMR imaging, updated neuronavigation, comprehensive neurophysiological monitoring, neurochemical monitoring with 5-aminolevulinic acid (5-ALA), and histopathological monitoring with multiple microscopic investigations of the resected tissue using frozen sections. Awake craniotomy and/or intraoperative cortical and subcortical brain mapping were performed if indicated. The main goal of surgery was defined as maximum possible removal of the contrast-enhanced area identified on preoperative T_1-weighted MR imaging without the risk of postoperative major permanent neurological morbidity. The final histopathological diagnosis of glioblastoma was established according to the current World Health Organization criteria[21] using paraffin-embedded tissue sections stained with hematoxylin and eosin and appropriate antibodies for immunohistochemistry.

Evaluation of the resection rate was based on visual side-by-side comparison of the preoperative and postoperative MR images obtained within 3 days after the surgery, using a 1.5 T clinical scanner (ExcellArt; Toshiba Medical Systems, Tokyo). Any contrast-enhanced area on T_1-weighted images was considered to be residual tumor.[8] In the analyzed cohort, the resection rate was 100% in 22 patients, and between 95% and 99% in the other 21 patients.

All patients underwent postoperative FRT, which was initiated within 2 to 3 weeks after surgical removal of the tumor. The treatment protocol was based on the three-dimensional planning system. The total dose was 60 Gy delivered in 30 fractions (2 Gy per fraction) in all cases. During the initial 25 fractions (up to 50 Gy of irradiation), the clinical target volume (CTV) was defined as the hyperintense area on T_2-weighted MR images and the 15 mm marginal area of the adjacent cerebral tissue. From 26 to 30 fractions (from 52 to 60 Gy of irradiation), the CTV was reduced to the resection cavity and the 15 mm marginal area of the adjacent cerebral tissue. Any contrast-enhanced area on T_1-weighted MR images was always included in the irradiation field. Concomitant and adjuvant chemotherapy was administered in 25 patients according to the standard protocols for nimustine (ACNU)[40,48] (9 cases) or temozolomide[46,47] (16 cases). Chemotherapy was omitted in 18 patients, but treatment with autologous formalin-fixed tumor vaccine (AFTV) concomitant with FRT was performed.[29]

Follow-up evaluations were performed by the attending neurosurgeon, starting 2 weeks after completion of FRT, and scheduled every 2–3 months thereafter. Additional examinations were done if required by the clinical condition of the patient. The regular investigations included physical testing with evaluation of KPS score and determination of the

Medical Research Council neurological functional grade, blood and urinary tests, and brain MR imaging with contrast medium. Other investigations were not performed unless were clinically indicated. The length of follow up varied from 3 to 71 months (median 17 months).

The diagnosis of tumor recurrence was based on the joint opinions of the neurosurgeon and neuroradiologist, and was defined as appearance of new contrast-enhanced lesion(s) on T_1-weighted MR images, or 25% or more increase of the volume of the previous enhanced lesion(s). Patterns of recurrence were considered as regional (in the wall of the resection cavity), marginal (within 20 mm from the margin of the resection cavity), distant (more than 20 mm from the margin of the resection cavity), multiple (several recurrences in various brain areas), and subarachnoid dissemination (Fig. 1). At the time of tumor recurrence the patients usually underwent salvage treatment, which included re-resection of the tumor, stereotactic radiosurgery, chemotherapy, vaccine therapy, or various combinations.

Clinical factors in the defined groups of patients were compared with the chi-square test or Mann-Whitney test. Overall (OS) and progression-free survival (PFS) were evaluated from the day of surgery and were compared with the log-rank test after construction of the Kaplan-Meier curves.

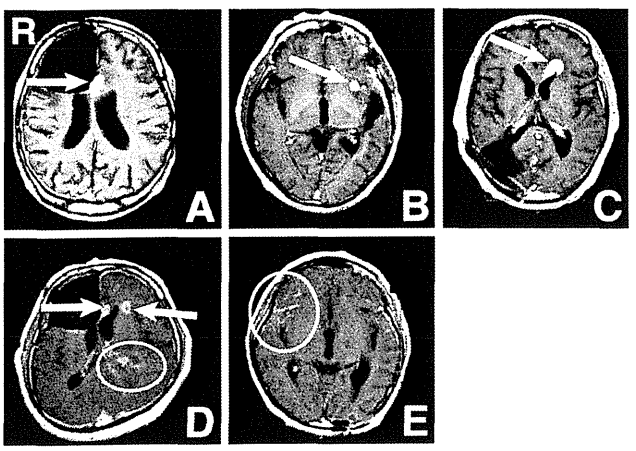

Fig. 1 T_1-weighred magnetic resonance images with contrast medium illustrating the patterns of glioblastoma recurrence (*arrows* and *circles*) after aggressive surgery and adjuvant management. A: regional, in the wall of the resection cavity; B: marginal, within 20 mm from the margin of the resection cavity; C: distant, more than 20 mm from the margin of the resection cavity; D: multiple, several recurrences in various brain areas; and E: subarachnoid dissemination.

Results

Tumor recurrence was observed during the follow-up period in 33 of 43 patients. Incidences of various recurrence patterns are presented in Table 1. Overall tumor progression within the wall of the resection cavity or within 20 mm from the margin accounted for 51% of cases. Subarachnoid dissemination was evident in 5 patients and was isolated pattern of recurrence in 3 of them. It was identified in 3 of 25 cases when the cerebral ventricle was opened during surgery, and in 2 of 18 cases when this was not done ($p = 0.78$). Spinal dissemination was evident in 1 patient, and no case of glioblastoma metastasis outside the central nervous system was identified.

PFS did not differ significantly between patients with regional or marginal progression of glioblastoma (22 cases) and patients with distant or multiple recurrences (8 cases), as shown in Fig. 2. Comparison of the investigated clinical factors did not differ

Table 1 Incidence of various recurrence patterns after aggressive surgery and adjuvant management of intracranial glioblastoma

Recurrence pattern	No. of cases*
Regional (in the wall of the resection cavity)	20 (46.5%)
Marginal (within 20 mm from the margin of the resection cavity)	2 (4.7%)
Distant (more than 20 mm from the margin of the resection cavity)	4 (9.3%)
Multiple (several recurrences in various brain areas)	4 (9.3%)
Subarachnoid dissemination	3 (6.9%)

*In 10 cases, recurrence of the tumor was not observed during follow-up period.

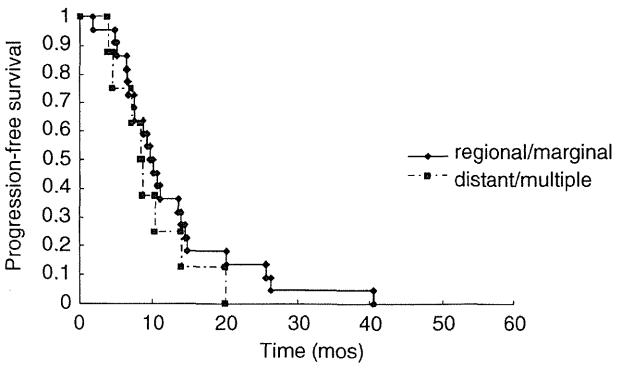

Fig. 2 Comparison of progression-free survival from the time of surgery in patients with different recurrence patterns of intracranial glioblastoma. There is no significant difference ($p = 0.27$).

Table 2 Comparison of clinical factors and outcome variables in patients with different recurrence patterns of intracranial glioblastoma

Clinical factors and outcome variables	Patients with regional or marginal progression (N = 22)	Patients with distant or multiple recurrences (N = 8)	p Value
Sex			0.35*
men	15	5	
women	7	3	
Age			0.70*
<50 yrs	10	3	
≥50 yrs	12	5	
Median age (range), yrs	52 (18–68)	56 (36–79)	0.16**
KPS score			0.21*
80–100	18	4	
60–70	1	2	
≤50	3	2	
Tumor location			0.24*
frontal	11	2	
temporal	6	4	
parietal	2	2	
occipital	1	0	
other	2	0	
Tumor side			0.23*
left	12	2	
right	10	6	
RPA class			0.29*
III	7	2	
IV	11	2	
V	4	4	
Resection rate			0.41*
100%	10	5	
95–99%	12	3	
Adjuvant treatment			0.70*
chemotherapy (ACNU or TMZ)	10	3	
vaccine therapy	12	5	
Salvage treatment			
any	14	6	0.56*
re-resection	8	0	0.05*
gamma knife radiosurgery	0	1	0.09*
chemotherapy (TMZ)	13	6	0.42*
vaccine therapy	1	0	0.54*
Outcome			0.29*
dead	15	7	
alive	7	1	
Overall survival			0.04***
median (range), mos	27 (3–57)	14 (6–23)	
actuarial 1-yr rate (95% CI)	90% (78–100%)	75% (45–100%)	
actuarial 2-yr rate (95% CI)	54% (32–76%)	0%	
Progression-free survival			0.27***
median (range), mos	10 (2–41)	8 (4–20)	
actuarial 1-yr rate (95% CI)	36% (16–56%)	25% (0–55%)	
actuarial 2-yr rate (95% CI)	14% (0–28%)	0%	

According to *chi-square test, **Mann-Whitney test, and ***log-rank test. ACNU: nimustine, CI: confidence interval, KPS: Karnofsky performance status, RPA: recursive partitioning analysis, TMZ: temozolomide.

significantly between the two defined groups (Table 2). No correlation between tumor location and recurrence pattern was found, but the recurrent tumor affected genu of the corpus callosum in all 4 patients with glioblastoma initially located in the prefrontal region (Fig. 3). In contrast, no neoplasm located in the parietal and/or occipital lobes recurred in the splenium of the corpus callosum.

Salvage treatment was performed in 14 of 22 patients with regional or marginal tumor progression and in 6 of 8 patients with distant or multiple recurrences ($p = 0.56$). However, re-craniotomy and additional lesion resection were done only in 8 cases of the former group ($p = 0.05$). Histopathological investigation revealed pure recurrence of the neoplasm in 6 cases, and intermixture with radiation necrosis in 2. Patients with regional or marginal progression of glioblastoma, who underwent re-resection of the neoplasm, had a mild tendency to better OS (median 13 vs. 10 months after diagnosis of recurrence), but the difference did not reach statistical significance (Fig. 4).

At the time of data analysis, 18 patients remained alive, whereas 25 had died, all of the intracranial tumor. OS was longer in patients with regional or marginal progression of glioblastoma compared to patients with distant or multiple recurrences ($p = 0.04$), as shown in Fig. 5.

Discussion

The conventional objectives of resective surgery for malignant glioma include relief of compression of the tumor bulk on the surrounding brain (important for neurological improvement), reduction of the volume of the neoplasm (increases the efficacy of adjuvant postoperative treatment), and establishment of the precise histopathological diagnosis (required for choice of the appropriate therapy, optimal follow up, and prediction of prognosis).[1] Additionally, extensive removal of the neoplasm may positively influence the survival. While the latter has not been formally proved to date,[38] there is a growing agreement that total resection of the lesion is associated with better long-term outcome. Adjustment for biases of age and eloquent area location in the dataset of randomized study on use of neurochemical navigation with 5-ALA during resection of glioblastoma found that median OS after complete removal of the enhanced lesion was significantly longer compared to cases with incomplete resection (17 months vs. 12 months).[45] In concordance, the report on European Organisation for Research and Treatment of Cancer randomized trial of combined chemotherapy for anaplastic gliomas showed the OS